Case Report

Liver enzyme elevation caused by a compression of infiltrative lipoma in a dog

Manabu Kurihara[a,*], Robert J. Bahr[b], Ronald Green[c]

[a] Massey University Veterinary Teaching Hospital, Private Bag 11-222, Palmerston North 4442, New Zealand
[b] Department of Veterinary Clinical Sciences, Center for Veterinary Health Sciences, Oklahoma State University, United States
[c] Institute of Veterinary, Animal & Biomedical Sciences, Massey University, Tennent Drive, Palmerston North 4474, New Zealand

1. Introduction

Adipose masses, especially lipoma, are considerably common in veterinary medicine. The current WORLD HEALTH ORGANIZATION (WHO) classification of mesenchymal skin and soft tissue tumors of domestic animals recognizes three benign forms of the adipose tissue, represented by lipoma, infiltrative lipoma and angiolipoma, and one malignant form, represented by liposarcoma [1].

Infiltrative lipoma was first reported in veterinary medicine in 1979 [2]. Infiltrative lipomas differ from malignant adipose tissue mass as in liposarcoma, but they show a more aggressive behavior by invading adjacent structures such as muscle, fasciae, spinal cord, joint capsule and cervical bone [3–9]. The reported local recurrence rate of infiltrative lipoma is high, ranging from 36 to 50% [10,11]. On the other hand, lipoma is a benign, soft, encapsulated, moderately discrete neoplasm consisting of differentiated fat cells, which seldom recur after surgery. Fibrolipoma and angiolipoma are uncommon variants of lipoma, being classified and diagnosed histopathologically. Fibrolipoma contains adipose tissue and bundles of collagenous connective tissue. Angiolipoma is composed of mature adipose tissue mixed with variable numbers of blood vessels [12].

The cells of a simple lipoma and infiltrative lipoma are histologically similar. Well-differentiated unilocular fat cells infiltrate the tissues, causing separation of fibers and atrophy [11]. Therefore, Infiltrative lipomas cannot be diagnosed accurately with either a fine-needle aspiration or a Tru-Cut biopsy. Aspiration cytology was performed on 16 infiltrative lipomas, and in each instance the cytologic diagnosis was lipoma, not infiltrative lipoma [10].

In this case, a large infiltrative lipoma invaded the adjacent tissue and compressed the left liver lobe, causing liver enzyme elevation. To the authors' knowledge, an elevation of liver enzymes is caused by a compression of infiltrative lipoma and pathologic findings of the compressed liver have not been reported.

2. Case details

A 13-year-old 2.0 kg intact female Chihuahua dog was evaluated because of lethargy, anorexia and vomiting. On physical examination, the dog was thin (body condition score, 3/9), bright, alert and responsive, estimated to be 5%–8% dehydrated and had a normal body temperature (38.0 °C). A systolic heart murmur (grade III/VI) over the left cardiac apex was detected, with no arrhythmia and a heart rate of 130 beats/min. Auscultation of the thorax revealed normal lung sounds. Mucous membranes were pink. No other abnormalities were detected on physical examination.

Hematologic evaluation revealed mild neutrophilic leukocytosis with no toxic changes (16,000 neutrophils/μL; reference range, 3000–12,500 leukocytes/μL). No other abnormalities were noted on CBC. Serum biochemical analysis revealed elevated liver enzymes (ALT 1305 U/L, AST 179 U/L and ALKP 565 U/L; reference range, 13–100 U/L, 1–37 U/L and 5–25 U/L, respectively), and elevated total bilirubin (0.8 mg/dL; reference range, 0.1–0.6 mg/dL), azotemia and hypercreatininemia (46 mg/dL and 1.7 mg/dL; reference range, 7–32 mg/dL and 0.5–1.6 mg/dL, respectively). Abdominal radiography performed by the referring veterinarian revealed suspected a adipose tissue mass in the left cranial abdomen. Abdominal ultrasound and computed tomography (Fig. 1) were carried out to evaluate the cause of clinical signs and elevated liver enzymes.

3. Diagnostic imaging findings and interpretation

An ultrasound examination of the mass was performed prior to the CT exam. The ultrasound findings showed a homogeneously hyperechoic mass in the left cranial abdomen, consistent with fat. The left lobe of the liver and the left kidney were displaced by the mass, compared with a normal position of these organs. However, the echogenicity of the entire liver was normal. Other findings of the abdominal ultrasound were within normal limits. An ultrasound-guided fine-needle aspiration of the mass was performed and cytology was indicative of lipoma.
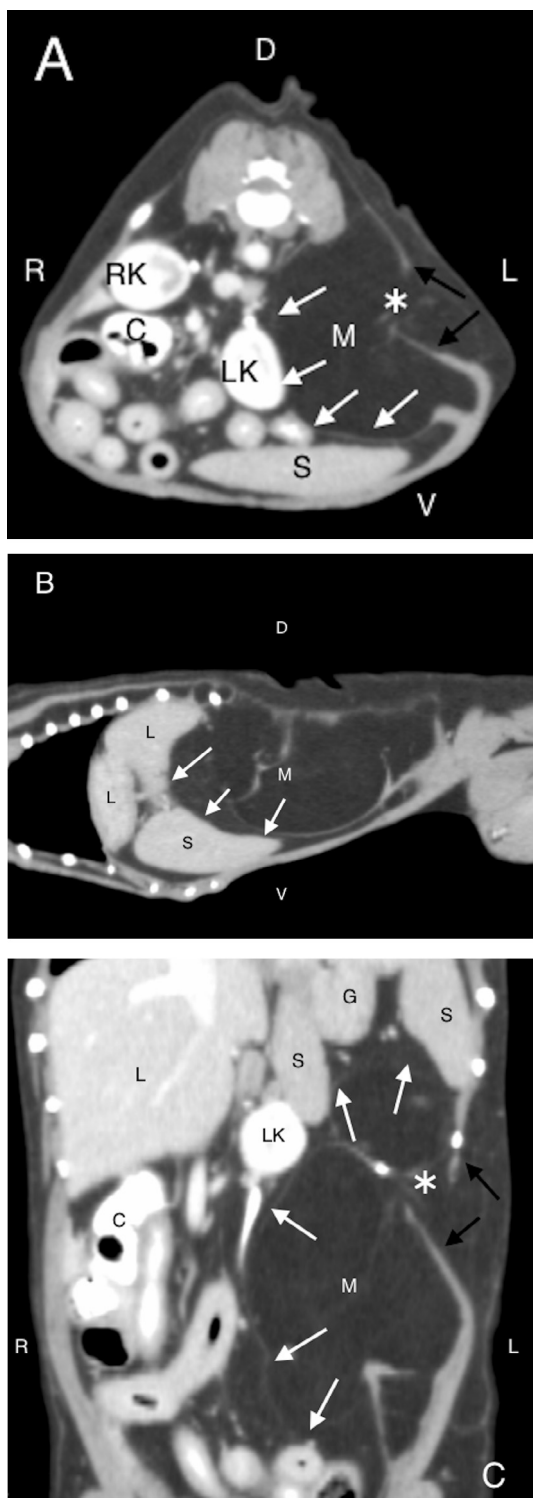
Fig. 1. Transverse post-contrast abdominal CT image at the level of the kidneys (A), Reformatted, left parasagittal post-contrast plane image (B), and a reformatted, dorsal post-contrast plane image (C), acquired with a soft tissue algorithm (window width, 330 Household Units [HU]; window level, 30 HU; slice thickness, 2 mm). (A): there is a large, fat-attenuating mass (M) that distorts and displaces the left kidney, spleen and other abdominal structures (white arrows). The mass separates the relationship of the internal and external abdominal oblique and transverse abdominis muscle layers (black arrows). Infiltration of the transverse abdominis muscle is visualized in the center of the muscular discontinuity (asterisk). (B): the mass causes cranioventral deviation of left lob of liver and spleen (white arrows). (C): the large fat-attenuating mass spreads across the left abdominal wall, displacing abdominal organs rightward. G = Stomach. LK = left kidney. RK = right kidney L = Liver. M = abdominal wall mass. S = Spleen. C = colon. D = Dorsal. L = Left. R = Right. V = Ventral.

A computed tomographic scan of the thorax and abdomen was performed under general anesthesia with a slice thickness of 2.0 mm and standard algorithm. A large fat-attenuating mass that measured 41.8 mm from cranial to caudal by 51.7 mm from medial to lateral by 43.3 mm from dorsal to ventral was noted in the left abdominal wall, causing the pronounced rightward deviation of the left lateral and medial hepatic lobe, left kidney, spleen and other abdominal structures. However, the difference between the compressed left lobe of the liver and normal positioning right lobe of the liver cannot be seen in terms of a mean CT value and contrast enhancement. The mass was homogeneous in attenuation, with a slightly ill-defined and irregular shape, and measured a mean CT value of −110 Hounsfield Units [HU] consistent with adipose tissue. A well-defined, linear, thin, soft tissue-attenuating (35 HU) septation was visualized within the mass, consistent with fibrous tissue or a residual layer of muscle tissue within the intramuscular space. This finding indicated discontinuity of the external and internal abdominal oblique muscle layers as well as of the transverse abdominis muscle layer by the mass. These CT findings suggested that the mass was infiltrative lipoma, separating the muscle continuity. There was no evidence of contrast enhancement of the mass or a metastatic process. The pre-contrast and contrast studies showed no evidence of a focal lesion in the liver or other abdominal structures. There were no abnormalities of the gallbladder or common bile duct. The ascending colon and cecum as well as some of small intestinal loops contain high-attenuating material in their lumen with no signs of GI obstruction. These findings are most likely caused by mineral-opaque foreign material in the small intestines and colon.

4. Treatment and outcome

Surgical excision of the large adipose tissue mass and infiltrated muscles including external and internal abdominal oblique muscles as well as of the transverse abdominis muscle was performed from a left flank laparotomy under general anesthesia. The macroscopic findings of the mass were homogenous, fat-like in appearance as well as partially encapsulated by the peritoneum in the deep side of the mass. There is no evidence of infiltrating the peritoneum. The mass had caused pressure atrophy of the abdominal wall muscles, partly infiltrating and separating the continuity of the abdominal wall muscle. After closing the surgical site, an ultrasound-guided Tru-Cut biopsy of the left lateral hepatic lobe was obtained. Three days later, after receiving general postoperative care in the hospital, the patient had an almost normal appetite and energy, and the liver enzymes were noted to be decreasing gradually. After discharging from the hospital (10 days later), all liver enzymes lessened, returning to a normal reference range. Liver enzymes were not repeatedly measured after normalization because the dog was clinically normal.

Histopathological findings of the mass were compatible with infiltrative lipoma, revealing that the mass was benign, well-differentiated adipose tissue surrounding the fibers of muscles. Clusters of the adipose cells infiltrated and separated the muscle fibers shrunken with dark cytoplasm and pyknotic nuclei. Evaluation of the margins of the mass confirmed complete resection (Fig. 2). The biopsied liver parenchyma showed non-specific findings such as moderate hepatocellular swelling and intrahepatic cholestasis as well as mild chronic changes such as regeneration of parenchyma, fibrosis, and ductular proliferation, following destruction of hepatic parenchyma.

Two years later, the dog died of cardiogenic pulmonary edema. Although postmortem was not performed, there was no clinical evidence of a recurrence of the infiltrative lipoma.

5. Discussion

Parenchymal disorders of the liver in dogs and cats can be grouped into seven categories: (1) reversible injury (cell swelling, excess glycogen accumulation, and lipidosis); (2) amyloidosis; (3) hepatocellular
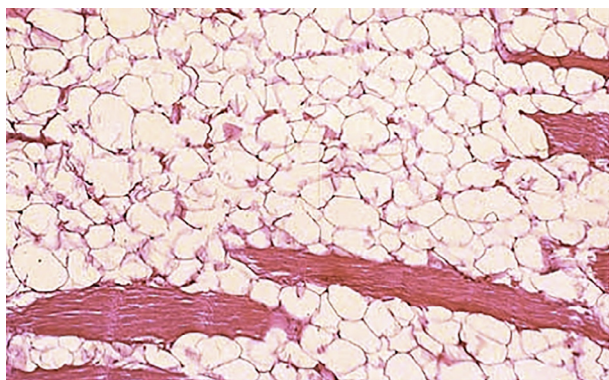
Fig. 2. Histopathology image reveals well-differentiated adipocytes infiltrating the adjacent muscle fibers as well as causing myodegeneration, consistent with the infiltrative lipoma. Hematoxylin and Eosin stain.

death, apoptosis, and necrosis; (4) acute and chronic hepatitis; (5) hepatic abscesses and granulomas; (6) hepatic metabolic storage disorders; and (7) miscellaneous conditions [13]. Generally, ALT and AST could be elevated by a direct physical compression from dilation of biliary canaliculus and/or hepatocellular injury secondary to cholestasis. ALKP is elevated by cholestasis directly and indirectly [14,15]. Likewise, neoplastic hepatic enzyme induction caused by osteosarcoma, mammary carcinoma and lymphoma is well known [16,17]. In the veterinary and human literature, hepatic biliary obstruction was caused by compression of abdominal masses such as pancreatic cyst and hepatic tumor [18–21]. In these reported cases, the extra-hepatic biliary duct obstruction was caused due to the abdominal masses adjacent to liver, which resulted in the intra-hepatic biliary duct obstruction and cholestasis. Finally, the hepatocellular injury was occurred by the bile acid accumulation of the intra-hepatic biliary duct. At the same time, the abdominal masses adjacent to liver directly compressed liver parenchyma induced the liver enzyme elevation owing to hepatocellular injury.

In this patient, the significantly elevated liver enzymes level is expected to be caused by the infiltrative lipoma. Although there is no sign of extra-hepatic biliary duct obstruction in the CT or ultrasound images, the enormous size of infiltrative lipoma pressing against and displacing the left lobe of the liver resulted in a physical compression of the hepatocellular structure. Based on the histopathologic findings such as hepatocellular injury and cholestasis, the hepatic enzymatic changes from these histopathologic changes were caused by the compression of the immense size of the infiltrative lipoma. Moreover, the liver enzymes level quickly lessened after the surgical excision of the infiltrative lipoma, which was a suggestion of the effect by the mass.

Although radiographic and ultrasonographic examinations are useful to determine a diagnosis of a lipomatous mass [22], these modalities are not efficient enough to determine the full extent of local invasion into surrounding tissues. They often cannot differentiate between lipoma and infiltrative lipoma. However, CT scans help in differentiating adipose tissue such as lipoma, infiltrative lipoma and liposarcoma [23,24]. Additionally, CT scans of patients with infiltrative lipoma are also helpful for surgical planning and radiation therapy planning in order to determine an infiltrative extent [25]. Therefore, CT is a useful modality for an adequate assessment of the extent of adipose masses and should be considered prior to surgery or irradiation if physical examination or other diagnostic processes cannot determine the adipose mass to be infiltrative or non-infiltrative.

Although there is nothing published concerning an infiltrative lipoma directly inducing liver enzyme elevation in the veterinary literature, secondary hepatopathy due to physical compression of an infiltrative lipoma, resulting in cholestasis and hepatocellular injury, is noted.

Competing interests

No conflicts of interest have been declared.

References

[1] Hendrick MJ. Tumors of adipose tissue. In: Hendrick MJ, Mahaffey EA, Moore FM, Vos JH, Walder EJ, editors. Histological classification of mesenchymal tumors of skin and soft tissues of domestic animals. Washington, D.C.: Armed Forces Institute of Pathology in cooperation with the American Registry of Pathology and the World Health Organization Collaborating Center for Worldwide Reference on Comparative Oncology; 1998. p. 11–60.

[2] Gleiser CA, Jardine JH, Raulston GL, Gray KN. Infiltrative lipoma in the dog. Vet Pathol 1979;16:623–4.

[3] Morgan LW, Toal R, Siemering G, Gavin P. Imaging diagnosis – infiltrative lipoma causing spinal cord compression in a dog. Vet Radiol Ultrasound 2007;48:35–7.

[4] Agut A, Anson A, Navarro A, Murciano J, Soler M, Belda E, et al. Imaging diagnosis-infiltrative lipoma causing spinal cord and lumbar nerve root compression in a dog. Vet Radiol Ultrasound 2013;54:381–3.

[5] Jennifer L, O'Driscoll, John JM. What is your neurologic diagnosis? J Am Vet Med Assoc 2006;229:933–5.

[6] Miller JA, Urie BK, Green EM. What is your diagnosis? J Am Vet Med Assoc 2014;245:43–4.

[7] Mullins RA, Bergamino C, Kirby BM. What is your diagnosis? J Am Vet Med Assoc 2017;250:615–7.

[8] Kim HJ, Chang HS, Choi CB, Song YS, Kim SM, Lee JS, et al. Infiltrative lipoma in cervical bones in a dog. J Vet Med Sci 2005;67:1043–6.

[9] Frazier KS, Herron AJ, Dee JF, Altman NH. Infiltrative lipoma in a canine stifle joint. J Am Anim Hosp Assoc 1993;29:81–3.

[10] Bergman PJ, Withrow SL, Straw RC, Powers BE. Infiltrative lipoma in dogs: 16 cases (1981–1992). J Am Vet Med Assoc 1994;205:322–4.

[11] McChesney AE, Stephens LC, Lebel J, Snyder S, Ferguson HR. Infiltrative lipoma in dogs. Vet Pathol 1980;17:316–22.

[12] Liggett AD, Frazier KS, Styer EL. Angiolipomatous tumors in dogs and a cat. Vet Pathol 2002;39:286–9.

[13] Cullen JM. Summary of the world small animal veterinary association standardization. Committee guide to classification of liver disease in dogs and cats. Vet Clin North Am Small Anim Pract 2009;39:395–418.

[14] Center SA. Interpretation of liver enzymes. Vet Clin North Am Small Anim Pract 2007;37:297–333.

[15] Stockham SL, Scott MA. Enzymes. Fundamentals of veterinary clinical pathology. 2th ed. Iowa: Blackwell Publishing; 2008. p. 639–74.

[16] Ehrhart N, Dernell WS, Hoffmann WE, Weigel RM, Powers BE, Withrow SJ. Prognostic importance of alkaline phosphatase activity in serum from dogs with appendicular osteosarcoma: 75 cases (1990–1996). J Am Vet Med Assoc 1998;213:1002–6.

[17] Karayannopoulou M, Polizopoulou ZS, Koutinas AF, Fytianou A, Roubies N, Kaldrymidou E, et al. Serum alkaline phosphatase isoenzyme activities in canine malignant mammary neoplasms with and without osseous transformation. Vet Clin Pathol 2006;35:287–90.

[18] Yano T, Kobayashi T, Kuroda S, Amano H, Tashiro H, Ohdan H. Obstructive jaundice caused by a giant liver hemangioma with Kasabach-Merritt syndrome: a case report. Surg Case Rep 2015:93.

[19] Odemis B, Parlak E, Basar O, Yuksel O, Sahin B. Biliary tract obstruction secondary to malignant lymphoma: experience at a referral center. Dig Dis Sci 2007;52:2323–32.

[20] Marchevsky AM, Yovich JC, Wyatt KM. Pancreatic pseudocyst causing extrahepatic biliary obstruction in a dog. Aust Vet J 2000;78:99–101.

[21] Lamb CR, Simpson KW, Boswood A, Matthewman LA. Ultrasonography of pancreatic neoplasia in the dog: a retrospective review of 16 cases. Vet Rec 1995;137:65–8.

[22] Volta A, Bonazzi M, Gnudi G, Gazzola M, Bertoni G. Ultrasonographic features of canine lipomas. Vet Radiol Ultrasound 2006;47:589–91.

[23] Spoldi E, Schwarz T, Sabattini S, Vignoli M, Cancedda S, Rossi F. Comparisons among computed tomographic features of adipose masses in dogs and cats. Vet Radiol Ultrasound 2017;58:29–37.

[24] Fuerst JA, Reichle JK, Szabo D, Cohen EB, Biller DS, Goggin JM. Computed tomographic findings in 24 dogs with liposarcoma. Vet Radiol Ultrasound 2017;58:23–8.

[25] Entee MC, Thrall DE. Computed tomographic imaging of infiltrative lipoma in 22 dogs. Vet Radiol Ultrasound 2001;42:221–5.